Coordinated Upregulation of Oxidative Pathways and Downregulation of Lipid Biosynthesis Underlie Obesity Resistance in Perilipin Knockout Mice

A Microarray Gene Expression Profile

Fernando Castro-Chavez,[1,2] Vijay K. Yechoor,[1] Pradip K. Saha,[1] Javier Martinez-Botas,[1] Eric C. Wooten,[1] Saumya Sharma,[3] Peter O'Connell,[1] Heinrich Taegtmeyer,[3] and Lawrence Chan[1]

Obesity is a major risk factor for diabetes and heart disease. We previously reported that the inactivation of the gene for perilipin (*plin*), an adipocyte lipid droplet surface protein, produced lean and obesity-resistant mice. To dissect the underlying mechanisms involved, we used oligonucleotide microarrays to analyze the gene-expression profile of white adipose tissue (WAT), liver, heart, skeletal muscle, and kidney of *plin*$^{-/-}$ and *plin*$^{+/+}$ mice. As compared with wild-type littermates, the WAT of *plin*$^{-/-}$ mice had 270 and 543 transcripts that were significantly up- or downregulated. There was a coordinated upregulation of genes involved in β-oxidation, the Krebs cycle, and the electron transport chain concomitant with a downregulation of genes involved in lipid biosynthesis. There was also a significant downregulation of the stearoyl CoA desaturase-1 gene, which has been associated with obesity resistance. Thus, in response to the constitutive activation of lipolysis associated with absence of perilipin, WAT activated pathways to rid itself of the products of lipolysis and activated pathways of energy expenditure that contribute to the observed obesity resistance. The biochemical pathways involved in obesity resistance in *plin*$^{-/-}$ mice identified in this study may represent potential targets for the treatment of obesity. *Diabetes* 52:2666–2674, 2003

From the [1]Section of Diabetes, Endocrinology and Metabolism, Departments of Molecular & Cellular Biology and Medicine, Baylor College of Medicine, Houston, Texas; the [2]Department of Molecular Biology in Medicine, Civil Hospital of Guadalajara, University Center of Health Sciences, University of Guadalajara, Guadalajara, Mexico; and the [3]Division of Cardiology, University of Texas Houston Medical School, Houston, Texas.

Address correspondence and reprint requests to Lawrence Chan, MD, Departments of Medicine and Molecular & Cellular Biology, Section of Diabetes, Endocrinology and Metabolism, Baylor College of Medicine, One Baylor Plaza, Houston, TX 77030. E-mail: lchan@bcm.tmc.edu.

Received for publication 21 March 2003 and accepted in revised form 30 July 2003.

Additional information for this article can be found in a data supplement available at http://diabetes.diabetesjournals.org.

Cac, carnitine/acylcarnitine translocase; Cpt, carnitine palmitoyl transferase; Pdk, pyruvate dehydrogenase kinase; PPAR-α, peroxisome proliferator–activated receptor-α; SREBP-1, sterol regulatory element-binding protein-1; WAT, white adipose tissue.

Perilipin (*plin*) is a member of a family of proteins that coat the surfaces of intracellular neutral lipid storage droplets, mainly in adipocytes and in steroidogenic cells (1,2). Perilipin, in the basal state, prevents access of hormone-sensitive lipase to the lipid droplet (3) and is a major substrate of cAMP-dependent protein kinase in adipocytes (4). Specific hormonal or cytokine stimuli, such as catecholamines and tumor necrosis factor-α, activate lipolysis by phosphorylating perilipin, thereby allowing hormone-sensitive lipase to access the lipid droplet and initiate its lipolytic action (5,6).

Plin$^{-/-}$ mice are characterized by constitutive lipolysis, normal body weight despite an increase in food consumption, a lean body habitus, and smaller fat depots composed of small adipocytes (7,8). These mice display increased oxygen consumption and are resistant to diet-induced and genetic obesity (7).

To explain this phenotype, we hypothesized that there had to be significant changes in the expression of genes involved in pathways for substrate and energy metabolism. We further reasoned that although perilipin is expressed in adipocytes, there should be concomitant changes in other tissues that are important in whole-body metabolism, such as the liver, skeletal muscle, heart, and kidney, to explain the profound changes seen in *plin*$^{-/-}$ mice. To test these hypotheses, we performed oligonucleotide microarray analysis of the above tissues of *plin*$^{-/-}$ mice and compared the data with those obtained from their wild-type littermates. We show a concomitant and coordinated upregulation of multiple genes involved in oxidative catabolic pathways along with downregulation of genes regulating fatty acid synthesis in the *plin*$^{-/-}$ mice, suggesting that these findings may underlie its lean and obesity-resistant phenotype.

RESEARCH DESIGN AND METHODS

Animal groups. Two groups of 6- to 10-week-old male mice were used in this study with six perilipin knockout (*plin*$^{-/-}$) mice in one group and six littermate wild-type (*plin*$^{+/+}$) mice in the other. All animal protocols were approved by the Institutional Animal Care and Use Committee at Baylor College of Medicine.

Sample preparation. Five different tissues—WAT, liver, heart, skeletal muscle, and kidney—were isolated from each of the 12 mice, and total RNA

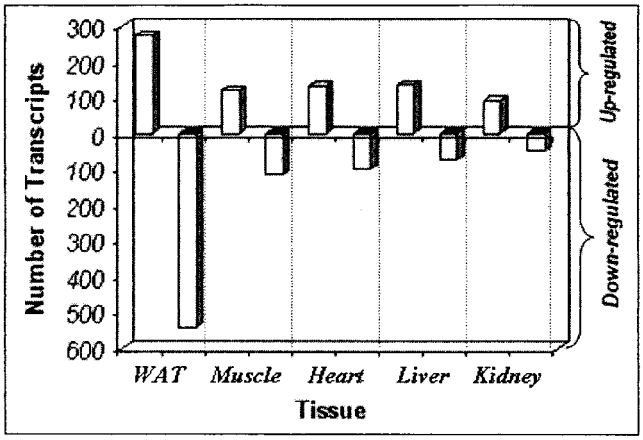

FIG. 1. Number of transcripts upregulated and downregulated per tissue in *plin*$^{-/-}$ mice compared with wild-type mice: 813 in WAT (270 increased, 543 decreased), 235 in muscle (121 increased, 114 decreased), 232 in heart (133 increased, 99 decreased), 209 in liver (137 increased, 72 decreased), and 140 in kidney (92 increased, 48 decreased).

was extracted from them using the Trizol (Invitrogen, Carlsbad, CA) reagent. To decrease variability introduced by individual biological differences, we made two sets of RNA. In the first set, equal amounts of total RNA were pooled from three mice per tissue for each group (pooled set). In the second set, we used the individual total RNA extracted from each tissue of the remaining three mice in each group (nonpooled set). We thus had four samples for each tissue per group (one pooled and three nonpooled). For the *plin*$^{-/-}$ WAT and heart, we had only three samples (one pooled and two nonpooled). These were then used to generate biotinylated cRNA according to the protocols provided by Affymetrix (Santa Clara, CA).

Gene expression assays and data analysis. A hybridization mixture containing 15 μg of the labeled cRNA was hybridized to Affymetrix MG-U74A-v2 chips, which were then washed, scanned, and analyzed. The chips were evaluated and subjected to global scaling as described elsewhere (9). The background and the scaled noise of each chip were averaged, and the means and SD of all expression intensities were calculated for the two groups (*plin*$^{-/-}$ versus *plin*$^{+/+}$). The results obtained from these five tissues were analyzed with the Affymetrix Genechip MAS V.5.0 and with dChip V.1.2 (10) software. For the perfect-match/mismatch (PM/MM) model (10), we applied four filters to screen for significantly altered gene expression between these two groups: *1*) 0.2 < SD/mean < 10; *2*) experiment-KO/basal-WT (E/B) or B/E >1.2, *3*) E-B or B-E >255, where 255 was the average scaled noise (9), and *4*) $P < 0.05$. To extend the reliable detection limit of expression in WAT, we also used the PM-only model (dChip V.1.2) using the same filters, as the PM-only model is immune to the adverse effect of the cross-hybridization experienced by some of the MM probes (online appendix 1 [available at http://diabetes.diabetesjournals.org]). Only results that showed a statistically significant difference between *plin*$^{-/-}$ and wild-type transcripts by this microarray analysis are presented. An alternative quantification method using fluorescence-based one-step RT-PCR (see below) applied to selected transcripts (online appendix 2) produced data that were concordant with that obtained by microarray analysis.

Quantitative RT-PCR. Quantitative real time RT-PCR reactions were carried out for selected genes using gene-specific primers either with SYBR Green or with specific fluorescent probes. Pooled and individual total RNA samples from the WAT of the *plin*$^{-/-}$ and littermate *plin*$^{+/+}$ mice was used as a template. The SYBR Green reactions were performed using the ABI Prism 7700 Sequence Detection System (Applied Biosystems, Foster City, CA) or DNA Engine Opticon (MJ Research, Reno, NV) and LightCycler-RNA Master SYBR Green I kit (Roche, Mannheim, Germany) and specific primers (sequences available on request) for each of the selected genes (online appendix 2). After initial RT temperature of 61°C for 20 min, denaturation for 2 min at 95°C followed by 40 cycles of denaturation at 95°C, primer annealing at 55°C and extension at 72°C, each for 22 s, were carried out with fluorescence detection done in the extension phase of each cycle. A melting curve analysis was performed to confirm the specificity of the amplification. The results were quantified after normalizing to transferrin in each of the samples. A similar reaction was carried out using specific fluorescent probes as described earlier (11) for selected genes, and the results were normalized to cyclophilin in each of the samples.

Gene annotations. Genes were annotated using public and Affymetrix databases. To detect metabolic pathways we also used MAPP-Finder V.1.0 and GenMAPP V.1.0 software (12,13).

RESULTS AND DISCUSSION

General expression profile of *plin*$^{-/-}$ and *plin*$^{+/+}$ mice. Of the 12,488 genes and expressed sequence tags represented on the MG-U74A v.2 oligonucleotide array, transcripts were deemed to be significantly up- or downregulated in the *plin*$^{-/-}$ mice (Fig. 1, Table 1) when they met the criteria defined in GENE EXPRESSION ASSAYS AND DATA ANALYSIS. This analysis was performed for each of the tissues studied.

As expected, WAT displayed the greatest changes in gene expression (Table 1). Expression patterns of genes for entire metabolic pathways were altered in *plin*$^{-/-}$ mice. The major pathways that were affected include β-oxidation, the Krebs cycle, and the electron transport chain

TABLE 1
Functional categorization of transcripts differentially expressed in *plin* mice tissues

	Gene expression change by tissue									
	WAT		Kidney		Liver		Heart		Muscle	
Functional categories	−	+	−	+	−	+	−	+	−	+
Transcription/translation	179	28	8	17	16	17	21	20	23	21
Signaling	55	24	7	21	7	30	10	20	11	26
Metabolism	25	41	6	15	15	7	10	20	17	11
Cell cycle and apoptosis	53	21	6	4	6	3	4	5	6	5
Defense response	19	43	2	11	2	18	1	12	2	5
Transport/trafficking	31	20	4	8	9	7	5	16	13	11
Structural	23	3	2	5	2	7	9	6	5	7
Membrane	23	12	2	4	3	16	3	5	10	7
Proteasome/protease	14	15	0	3	4	6	2	5	3	4
Ribosomal	7	5	1	0	0	1	6	1	0	2
Others	39	23	3	0	3	12	13	8	10	7
Unknown	35	15	7	2	0	6	1	0	4	3
Expressed sequence tags	40	13	0	2	5	5	12	7	8	9
Secreted	0	7	0	0	0	2	2	8	2	3
Total	543	270	48	92	72	137	99	133	114	121

The number of transcripts that are significantly upregulated (−) or downregulated (+) in the *plin*$^{-/-}$ mice in each tissue are listed.

TABLE 2
Upregulation of fatty acid oxidation and downregulation of lipid synthesis–related genes in *plin*$^{-/-}$ mice

Gene ID	Gene/protein name (symbol)	Fold change	Tissue
Upregulated in fatty acid degradation (β-oxidation)			
U01170	Carnitine palmitoyltransferase 2 (Cpr2) *	2.25	W
AB017112	Carnitine/acylcarnitine translocase (Cac) *	2.26	W
AB017112	Carnitine/acylcarnitine translocase (Cac)	1.68	*h*
AB015800	Organic cation/carnitine transporter 2 (Octn2)	1.71	*k*
AF030343	Enoyl CoA hydralase 1 (Ech1)	1.91	W
AI844846	2,4-Dienoyl CoA reductase 1 (Decr1)†	1.91	W
AW012588	3-Ketoacyl-CoA thiolase B (Kat) *	1.89	W
Downregulated in fatty acid degradation			
Z31689	Lysosomal acid lipase 1 (Lip1)	−1.88	*l*
AB017112	Carnitine/acylcarnitine translocase (Cac)	−1.82	*m*
Downregulated in fatty acid biosynthesis/ cholesterol biosynthesis			
M21285	Stearoyl CoA desaturase 1 (Scd1)	−4.00	W
M21285	Stearoyl CoA desaturase 1 (Scd1)	−5.34	W
M21285	Stearoyl CoA desaturase 1 (Scd1)	−3.56	*m*
AV327760	Stearoyl CoA desaturase 2 (Scd2)†	−2.35	W
M26270	Stearoyl CoA desaturase 2 (Scd2)†	−3.29	W
AV327760	Stearoyl CoA desaturase 2 (Scd2)	−1.63	*k*
AI314696	Stearoyl CoA desaturase 1-like (Scdl-1)	−5.03	W
AW121639	ATP citrate lyase homolog (Acly)†	−2.33	W
AW122523	Long-chain fatty-acyl elongase (Lce)	−20.68	W
AA619207	Fatty acid CoA ligase long chain 4 (Facl4)	−3.12	W
AA716963	Isopentenyl diphospate δ isomerase (Idil)	−7.70	W
D42048	Squalene epoxidase (Sqle)	−1.98	W
AW122260	Lanosterol 14-α-demethylase (Cyp51)	−2.10	W
AI848668	Sterol-C4-methyl oxidase-like (Sc4mol)	−3.1	W
AB030505	Androgen regulated homolog (Arsdrl)	−2.11	W
AF042491	Progesterone receptor component 1 (Pgrmcl)†	−3.28	W
U96116	Hydroxysteroid dehydrogenase10 (Hsd17b10)	−1.38	*k*
AB017026	Oxysterol binding protein-like 1A (Osbpl1a)	−2.56	*m*
U37545	Steroid sulfatase (Sts)	−2.01	*l*
AB010266	Steroid 21 hydroxylase (Cyp21a1)	−4.60	*l*

Genes with significant changes in *plin*$^{-/-}$ mice from various tissues are represented, with the fold changes and the tissue showing the change in the last two columns. The first Scd1 and Scd2 transcripts in WAT represent the probe target site nearest to the 3′ end, whereas the second ones are closer to the 5′ end. W, WAT; *k*, kidney; *l*, liver; *h*, heart; *m*, muscle; *genes whose expression was also measured using quantitative real-time RT-PCR as shown in online appendix 2; †genes found using the PM-only model as shown in RESEARCH DESIGN AND METHODS.

(Tables 2 and 3, Fig. 2). Many genes involved in transcription and translation regulation were also downregulated in *plin*$^{-/-}$ WAT, accounting for 33% of all its downregulated transcripts. All of the genes that are significantly changed in *plin*$^{-/-}$ WAT are listed in online appendix 3.

β-Oxidation genes are upregulated in *plin*$^{-/-}$ mice. The rate-limiting step for β-oxidation of long-chain fatty acids is their transport across the inner mitochondrial membrane via the carnitine palmitoyl transferase (Cpt) and carnitine/acylcarnitine translocase (Cac) system. Both *Cpt2* and *Cac* genes were significantly upregulated in the *plin*$^{-/-}$ mice. The transcripts of two of the three enzymes involved in β-oxidation, namely, 3-ketoacyl-CoA thiolase B and enoyl CoA hydratase, were also significantly upregulated in the WAT of *plin*$^{-/-}$ mice. The mRNA for 2,4-dienoyl CoA reductase 1, which is involved in the oxidation of unsaturated fatty enoyl-CoA esters (that have double bonds in both odd- and even-numbered positions before their further degradation via β-oxidation), was also upregulated significantly in the *plin*$^{-/-}$ mice. In kidney, where it has the strongest expression, the gene for the organic cation/carnitine transporter 2 (Octn2 or Slc22a5) was also upregulated. This transporter is involved in an active sodium-dependent high-affinity cellular uptake of carnitine. Thus, in the WAT of *plin*$^{-/-}$ mice, there is a coordinated upregulation of multiple genes regulating fatty acid oxidation (Fig. 2).

Fatty acid/cholesterol biosynthesis genes are decreased in *plin*$^{-/-}$ mice. Multiple transcripts of fatty acid/cholesterol biosynthesis-related pathways were downregulated in WAT; a few of these transcripts were also downregulated in muscle, kidney, heart, and liver (Table 2). In WAT, the transcript for ATP citrate-lyase, the primary enzyme responsible for the synthesis of cytosolic acetyl-CoA, which plays a central role in de novo lipid biosynthesis, was decreased. Transcripts for members of the Scd family, which are involved in a rate-limiting step in the synthesis of monounsaturated fatty acids (see below), were also significantly decreased in WAT of the *plin*$^{-/-}$ mice (Fig. 3).

The mRNAs for fatty-acyl CoA ligase long chain 4 and for long-chain fatty-acyl elongase were also decreased in the *plin*$^{-/-}$ mice. The former activates long-chain fatty acids for the synthesis of cellular lipids that preferentially

TABLE 3
Upregulation of Krebs cycle– and electron transport–related genes in *plin*$^{-/-}$ mice

Gene ID	Gene/protein name (symbol)	Fold change	Tissue
Upregulated in Krebs cycle and related reactions			
U68564	Isocitrate dehydrogenase [NAD+] γ (Idh3g)	1.92	W
A1840979	Succinate-CoA ligase GDP-forming α (Suclg1)	1.81	W
NM_008617	Malale dehydrogenase mitochondrial (Mor1)†*	1.55	W
AI849904	Dihydrolipoamide succinyltransferase E2K (Dist)	1.72	*k*
AI849904	Dihydrolipoamide succinyltransferase E2K (Dist)	1.88	*h*
AV328137	Glutamate oxaloacetate transaminase 2 (Got2)	1.94	*h*
Downregulated in Krebs cycle and related reactions			
AW124813	Dihydrolipoamide S-acetyltransferase (Pdc-a2)	−1.43	*m*
AI835446	Isocitrate dehydrogenase 3 [NAD+] α (Idh3a)	−2.04	*m*
AW125431	Citrate synthase homologous (Cs)	−1.53	*m*
AF058955	Succinate-CoA ligase ADP-forming β (Sucla2)	−1.56	*m*
AA691492	Pyruvate dehydrogenase kinase 1 homolog (Pdk1)	−2.18	W
AA867881	Dihydrolipoamide S-acetyltransferase (Pdc-c2)	−2.02	W
Upregulated in electron transport (respiratory) chain			
AI846396	NADH dehydrogenase (ubiquinone) 1α 9 (Ndufa9)†*	1.61	W
AI845556	NADH dehydrogenase (ubiquinone) 1β 9 (Ndufb9)	1.54	W
AW046724	NADH dehydrogenase (ubiquinone) 1 α 1 (Ndufal)	1.62	*k*
AW121892	Cytochrome C-1 (Cycl)†	1.26	W
AA674669	Succinate dehydrogenase complex B-Ip (SdhB) *	2.09	W
AW125380	Ubiquinol-cytochrome C reductase 1 (Uqcrc1)	1.94	W
AF037370	Cytochrome C oxidase VIIa 1 (Cox7a1)†	1.43	W
U15541	Cytochrome C oxidase polypeptide VIII (Cox8b)	2.97	W
AV260484	Cytochrome C oxidase polypeptide VIII (Cox8b)	2.39	W
AW123987	Cytochrome C oxidase assembly protein 2 (Sco2)	2.89	W
L01062	ATP synthase, H^+ transporting, F1 α 1 (Atp5al)†	1.20	W
AA870675	ATP synthase, H^+ transporting, F1 γ 1 (Atp5cl)*	2.16	W
A1461702	ATP synthase, H^+ transporting, F0 γ 2 (Arp5c2)†	1.32	W
Downregulated in electron transport (respiratory) chain			
AI835051	NADH ubiquimone oxidoreductase homolog (Ndufs1)	−1.55	*m*
Upregulated in electron transport NADPH dependent			
M31775	Cytochrome b-245, α polypeptide (Cyba)	3.06	W
AW046124	Cytochrome b-245, α polypeptide (Cyba)	3.22	*l*
M31775	Cytochrome b-245, α polypeptide (Cyba)	1.78	*l*
U90535	Flavin containing monooxygenase 5 (Fmo5)	2.22	W
U59488	Neutrophil cytosolic factor 4, p40phox (Ncf4)	6.71	W
U12961	NADPH dehydrogenase, quinone 1 (Nqo1)	3.47	W
Downregulated in electron transport NADPH dependent			
M21856	Cytochrome P450 2b10 (Cyp2b10)	−1.71	*l*

The Krebs cycle and electron transport genes with significant changes in the *plin*$^{-/-}$ mice from various tissues are represented, with the fold changes and the tissue showing the change in the last two columns. *Genes whose expression was also measured using quantitative real-time RT-PCR as shown in online appendix 2; †genes found using the PM-only model as shown in RESEARCH DESIGN AND METHODS.

use arachidonate and eicosapentanoate as substrates, and the latter is involved in converting palmitic to stearic acid (14).

The mRNAs for a number of sterol biosynthetic enzymes were downregulated. These included the transcripts for isopentenyl diphosphate δ isomerase, which participates in the isoprenoid biosynthetic pathway, giving end products that include steroid hormones, bile acids, and cholesterol; squalene epoxidase, a potential target for lipid/cholesterol lowering therapies (15–17) that catalyzes the first oxygenation step in sterol biosynthesis; and lanosterol 14-α-demethylase (Cyp51), also a target in cholesterol therapy (18–20), which catalyzes the removal of the 14 α-methyl group from lanosterol, a critical step in the production of ergosterol in the cholesterol biosynthetic pathway (Fig. 3).

In the kidney, the gene for hydroxysteroid dehydrogenase 10, an oxidoreductase participating in lipid metabolism, was downregulated. In skeletal muscle, the transcript for oxysterol binding protein-like 1A was also downregulated. Oxysterol binding protein is an intracellular transporter of oxygenated derivatives of cholesterol from lysosomes to the nucleus, where they downregulate genes for the LDL receptor. In the liver, the mRNAs for steroid 21-hydroxylase and steroid sulfatase, which are involved in the conversion of sulfated steroid precursors, were also significantly downregulated (Table 2).

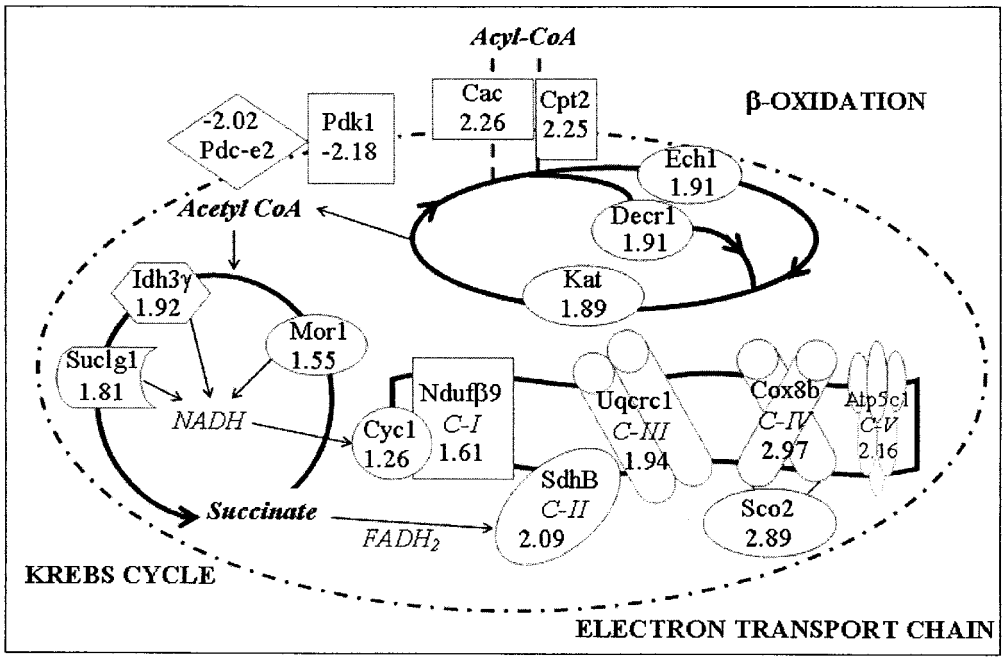

FIG. 2. Metabolic pathways altered in mouse *plin*$^{-/-}$ WAT: β-oxidation, Krebs cycle, and electron transport chain. Fold changes in transcript levels are listed beneath the gene symbols. Decr1, 2,4-dienoyl CoA reductase 1; Ech1, enoyl CoA hydratase 1; Kat, acetyl-CoA acyltransferase; Pdc-e2, dihydrolipoamide S-acetyltransferase; Idh3γ, isocitrate dehydrogenase [NAD]γ; Suclg1, succinate-CoA ligase GDP-forming α; Mor 1, malate dehydrogenase mitochondrial; Nduf β9, NADH dehydrogenase (ubiquinone) 1β9; SdhB, succinate dehydrogenase complex, B-Ip; Uqcrc1, ubiquinol-cytochrome C reductase 1; Cyc1, cytochrome C-1; Cox8b, cytochrome C oxidase polypeptide VIIIb; Sco2, cytochrome C oxidase assembly protein 2; Atp5c1, ATP synthase, H+ transporting, F1 γ 1. Substrates are shown in italics.

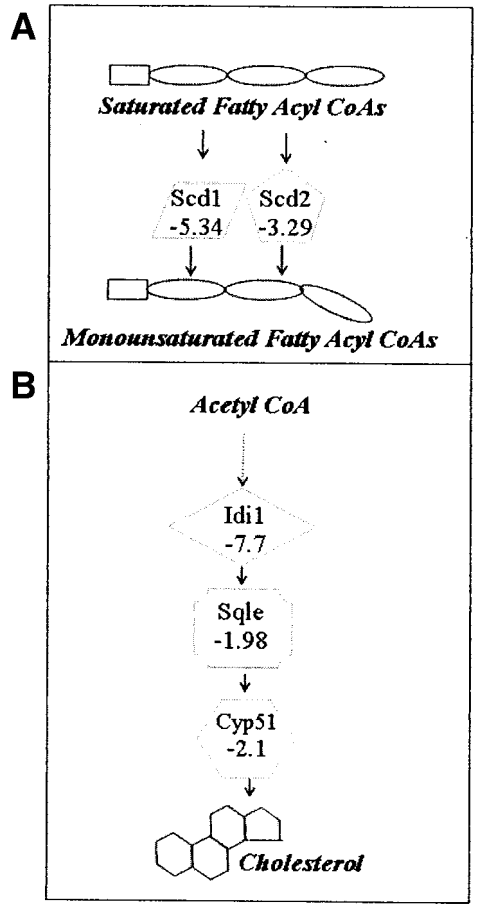

FIG. 3. Downregulation of transcripts involved in unsaturated fatty acid (*A*) and cholesterol biosynthesis (*B*) in *plin*$^{-/-}$ WAT. The fold change is listed beneath the gene symbols. Scd, stearoyl CoA desaturase; Idi1, isopentenyl diphosphate δ isomerase 1; Sqle, squalene epoxidase; Cyp51, lanosterol 14-α-demethylase (Ldm).

Transcripts for Scd enzymes are downregulated in *plin*$^{-/-}$ mice. A notable finding in *plin*$^{-/-}$ WAT was the coordinated downregulation of the stearoyl coenzyme A desaturase (Scd) genes Scd1 and Scd2 (Fig. 3, online appendices 4 and 5). Scd1 mRNA was expressed at a high level in WAT of wild-type mice and was significantly downregulated in *plin*$^{-/-}$ mice.

The Scd family, also known as δ-9-desaturase in humans and *asebia* in mice, is composed of iron-containing enzymes that catalyze a rate-limiting step in the synthesis of monounsaturated fatty acids by introducing the first double bond, mainly in oleate and palmitoleate. Scd expression is modulated by dietary factors (e.g., polyunsaturated fatty acids, cholesterol, vitamin A [21–23]), hormonal signals (e.g., insulin, glucagon [24]), environmental factors (e.g., temperature changes, thiazolinediones, metals, alcohol, phenolic compounds [25–28]), peroxisomal proliferators (29), and developmental processes (30). Altered Scd activity has been observed in a wide range of disorders, including diabetes, atherosclerosis, cancer, obesity, and viral infections (25,31,32).

The *plin*$^{-/-}$ mice are characterized by a ~60% decrease in total body lipid content but have the same body weight as their wild-type littermates, despite an ~30% increase in caloric intake (7). They also exhibit increased O_2 consumption, reflecting an increased metabolic rate compared with wild-type mice. A similar phenotype is evident in mice with Scd1 deficiency, occurring either for a natural mutation, as in the *asebia* mice (33), or as a result of gene targeting, as in the *scd1*$^{-/-}$ mice (34). They exhibit an ~50% decrease in adiposity with a normal body weight and an ~25% increase in their food intake, accompanied by an increase in their O_2 consumption. Furthermore, like the *plin*$^{-/-}$ mice, the *scd1*$^{-/-}$ mice show an upregulation of the fatty acid oxidation genes with a concomitant downregulation of the fatty acid synthesis genes. These parallel observations suggest that the downstream effects in both of these models, such as the relative or absolute increase in saturated fatty acids in the tissue, concomitant with a

decrease of unsaturated fatty acids in the absence of Scd1 (*scd1*$^{-/-}$ mice), or with a decrease in expression of both Scd1 and Scd2 in the *plin*$^{-/-}$ mice (Table 2), may contribute to some of the observed changes in these models. However, other changes in gene expression profile in the *plin*$^{-/-}$ mice and not reported in the *scd1*$^{-/-}$ mouse point to additional regulatory mechanisms that come into play in the *plin*$^{-/-}$ mice.

Sterol regulatory element-binding protein-1 (SREBP-1) has been postulated to be a regulator of Scd (35–37). In this study, we note a significant alteration in the expression of multiple members of the Scd gene family, all without a significant change in the expression of SREBP-1. Thus, it is likely that this downregulation of the Scd genes in the *plin*$^{-/-}$ mice occurs either downstream of SREBP-1 or via a separate regulatory pathway. SREBP-1–independent regulation of the expression of Scd1 by cholesterol has been reported previously (38,39). The transcripts for Scd1 and Scd2 together with a Scd1-like gene all were significantly downregulated in the WAT, and that for Scd1 in muscle and Scd2 in kidney were significantly downregulated in *plin*$^{-/-}$ mice (Table 2).

Transcript alignment by hierarchical clustering is useful to identify genes coordinately regulated and selectively expressed among different tissues. Hierarchical clustering (dChip V 1.2) shows that in *plin*$^{-/-}$ WAT, transcripts for Scd1 and Scd2, were present in the same cluster (online appendix 4). Transcripts for ATP citrate lyase, a major factor determining the level of cytosolic acetyl CoA (see below), also occurred in the same cluster, suggesting a coordinated downregulation for these genes. It is interesting that a similar clustering of these genes was seen in the leptin-regulated genes studied in leptin-treated wild-type WAT (40). Hierarchical clustering of five different tissues (WAT, liver, heart, muscle, and kidney) from both *plin*$^{-/-}$ and wild-type revealed the following genes as coordinately regulated by this analysis in relation to Scd: long-chain fatty acyl elongase clustered with Scd2, whereas pyruvate dehydrogenase kinase 1, aldehyde dehydrogenase 1A4, and eukaryotic translation initiation factor 1A clustered with Scd1, all being significantly downregulated in WAT of *plin*$^{-/-}$ mice (online appendix 5).

Krebs cycle genes are upregulated in *plin*$^{-/-}$ mice. The major portion of the energy from the oxidation of carbohydrates and fatty acids comes from the generation of reducing equivalents in the Krebs cycle and the subsequent generation of ATP via redox reactions of the electron transport chain. The Krebs cycle, fatty acid β-oxidation, and the electron transport-mediated ATP generation occur inside the mitochondria, whereas glycolysis, lipolysis, and fatty acid synthesis are cytosolic events. The mitochondrial membrane is impermeable to acetyl CoA, the common intermediate through which both glucose and fatty acids are fed into the Krebs cycle. For glucose to be converted into acetyl CoA, it is first converted to pyruvate in the cytosol through glycolysis. Pyruvate is transported and converted into acetyl CoA in the mitochondria by the pyruvate dehydrogenase complex, a key mitochondrial membrane-bound multisubunit enzyme.

The transcript for dihydrolipoamide S-acetyltransferase, the E2 component of the pyruvate dehydrogenase, was downregulated in *plin*$^{-/-}$ mice. This downregulation would be expected to inhibit the conversion of pyruvate into acetyl CoA and direct pyruvate to either oxaloacetate by pyruvate carboxylase or to lactate. However, there also was a decrease in the transcript of pyruvate dehydrogenase kinase 1 (Pdk1), which normally inhibits Pdh by phosphorylating the E1a component of the Pdh complex. In this context, it is important to note that the key enzyme in determining fuel selection has been postulated to be Pdk4 (41–43), whereas the role of Pdk1 in this process is unclear. Although Pdk4 transcript level was not changed significantly, its activity in the *plin*$^{-/-}$ mice is expected to be increased, as NADH is reportedly a strong activator of this enzyme (41), and intramitochondrial NADH levels are expected to be elevated in these mice as a result of the increased β-oxidation.

In addition to the above, transcripts for enzymes of the Krebs cycle, such as isocitrate dehydrogenase [NAD^+]γ, succinate-CoA ligase Gdp-forming α, succinate dehydrogenase, and malate dehydrogenase, all were upregulated in *plin*$^{-/-}$ mice (Fig. 2, online appendix 6). These four steps represent four of the five irreversible steps of the Krebs cycle; they catalyze reactions that generate reducing equivalents (NADH, FADH2) and GTP. Their upregulation suggests that the flux through the Krebs cycle is maintained at a higher level to keep up with the activated lipolysis and β-oxidation in the *plin*$^{-/-}$ mice.

In the *plin*$^{-/-}$ mice, with the increase in acetyl CoA generated from an activated β-oxidation, a rise in intramitochondrial citrate (the first intermediate generated in the Krebs cycle) would be expected. This increase would result in an increase in cytoplasmic citrate, because citrate is transported across the mitochondrial membrane via the tricarboxylate (citrate) carrier. Cytoplasmic citrate plays an important role in the regulation of both carbohydrate and lipid metabolism. Increased cytoplasmic citrate allosterically inhibits the rate-limiting step of glycolysis catalyzed by phosphofructo kinase-1, which is further inhibited by an increase in the cellular ATP/ADP ratio in these animals, as would be expected by the increased fatty acid oxidation and the activated Krebs cycle.

The citrate-malate shuttle is involved in transporting acetyl CoA, generated in the mitochondria, to the cytoplasm, where it acts as a precursor to malonyl CoA, the substrate of fatty acid synthesis. Once in the cytosol, citrate is broken down into oxaloacetate and acetyl CoA by ATP-citrate lyase, and the transcript for this enzyme was downregulated in the *plin*$^{-/-}$ mice. Hence, although intramitochondrial acetyl CoA levels may be increased in the *plin*$^{-/-}$ mice, this is not likely to be reflected in the cytoplasm, because of this downregulation. As a consequence, there would be a decrease in substrate available for acetyl CoA carboxylase, which generates malonyl CoA from acetyl CoA and with it a decreased precursor pool for fatty acid synthesis. In addition, the decrease in malonyl CoA would decrease the inhibition on Cpt and further stimulate an increase in β-oxidation. Furthermore, the higher levels of saturated fatty acids that may result from the decrease in Scd expression have been postulated to inhibit acetyl CoA carboxylase (34,44), further decreasing malonyl CoA and increasing β-oxidation.

Electron transport chain genes are upregulated in *plin*$^{-/-}$ mice. The mitochondrial electron chain is composed of five complexes, each consisting of multiple subunits. In the *plin*$^{-/-}$ mouse WAT, there was an upregulation of transcripts for at least one subunit of each of the five complexes of the electron transport chain (Table 3, Fig. 2, online appendix 6). The coordinated increase in these transcripts is in keeping with the demands of the increased flux of reducing equivalents generated by activated β-oxidation and the Krebs cycle. The consumption of molecular oxygen for oxidative metabolism mediated by the activation of the electron transport chain accounts for part of the increase in O_2 consumption observed in the *plin*$^{-/-}$ mice. However, these changes in WAT probably do not account for all of the increase in O_2 consumption seen in *plin*$^{-/-}$ mice (11 and 20% while on regular diet and high-fat diets, respectively) (7), as these changes were not reflected in skeletal muscle, which normally contributes to a larger portion of the total body O_2 consumption.

Changes in the transcript level of other metabolism regulating genes. Although we observed a 25% increase in the transcript level for peroxisome proliferator–activated receptor-α (PPAR-α) in this microarray analysis, this difference between *plin*$^{-/-}$ and wild-type WAT did not reach statistical significance. As PPAR-α regulates many of the genes involved in fatty acid oxidation and thus is a possible candidate to mediate many of the changes observed in *plin*$^{-/-}$ mice, we studied the expression of PPAR-α in these mice using real-time quantitative RT-PCR as a complementary approach. PPAR-α was seen to be significantly increased by fourfold in the *plin*$^{-/-}$ mice as compared with the wild-type controls (online appendix 2). A few other well-studied genes involved in lipid and carbohydrate metabolism, including leptin, resistin, and adiponectin, are notable for the lack of a significant difference in expression between *plin*$^{-/-}$ and wild-type mice.

Changes in the transcript level of other genes. Aquaporin 7, a water/glycerol channel in WAT, was upregulated in *plin*$^{-/-}$ mice. The PPAR-α target gene fasting-induced adipocyte factor, a novel endocrine signal involved in the regulation of lipid metabolism (34,45), was upregulated in *plin*$^{-/-}$ mice, as was observed in *Scd1*$^{-/-}$ mice (34). We also found that in the WAT of *plin*$^{-/-}$ mice, the transcripts for 6-phosphofructo-2-kinase/fructose-2,6-bisphosphatase 1 and triosephosphate isomerase were upregulated. Whereas in the WAT of *plin*$^{-/-}$ mice there was an upregulation of the transcripts for prostacyclin synthase (involved in prostacyclin synthesis) and that for 5-lipoxygenase activating protein (involved in leukotriene synthesis), there was a downregulation of the transcripts for phospholipase A2 and phospholipase A2 activating protein, both involved in the generation of arachidonate, the precursor substrate for all of the eicosanoids.

We observed in *plin*$^{-/-}$ WAT an increased expression of transcripts normally thought to be associated with leukocytes (Table 3). Among them are transcripts for NADPH-dependent electron transporters (46), together with the colony-stimulating factor 1 and 2 receptors, the transcription factor Pu1, recently reported as uniquely expressed in the stromal fraction isolated from wild-type and *ob/ob* adipose tissue (47), F4/80, and Mac-1β (48). Recently, the conversion of preadipocytes into macrophages has been demonstrated (48), whereas on the flip side, macrophages, which accumulate lipid and become foam cells in atherosclerotic plaques, have been found expressing adipophilin (49) and perilipin transcripts (50), pointing to the expression of common genes and regulatory pathways in these different cell types. However, these have to be interpreted cautiously as the WAT also has other nonadipose components, especially a vascular tissue component, which may contribute to a disproportionately higher leukocyte associated transcripts in the *plin*$^{-/-}$ mice, as a result of their lower relative adipose content. An annotated list of the genes for NADPH-dependent electron transporters is presented in online appendix 6. Transcripts of genes involved in heme synthesis, such as heme oxygenase (decycling) 1 and δ aminolevulinic acid synthase 1 and 2, were also increased in the *plin*$^{-/-}$ WAT.

Conclusion. We have previously shown that perilipin gene ablation leads to constitutively activated lipolysis, resulting in an increase in free fatty acids and glycerol in WAT (7). We now demonstrate mechanisms through which the *plin*$^{-/-}$ mice adapt to this altered metabolism by activating mechanisms to dispose of these lipolytic products through upregulation of oxidative catabolic pathways and downregulation of lipid/sterol synthetic pathways. This coordinated program of changes in oxidative catabolism and pathways of energy expenditure thus would underlie the obesity resistance observed in these mice.

Although perilipin has not been previously implicated in any transcriptional regulation, either directly or indirectly, we show that the disruption of perilipin leads to extensive changes in gene expression in the WAT. Because the constitutively activated lipolysis is the primary consequence of the lack of perilipin, the resultant increase in intracellular fatty acids and their subsequent oxidation products would be the most likely candidates to mediate many of the observed changes in these mice. Although the exact mechanism of nutrient sensing remains unclear, it is likely that these lipid intermediates may act as ligands, co-factors, or co-activators for transcription factors that are the effectors of the alterations observed in the global gene expression. Indeed, the observation that all of these metabolic pathways, with multiple components of each pathway, are coordinately changed argues strongly for a set of transcriptional factors or co-activators as mediators for some of the observed changes. It is interesting that the increased expression levels of PPAR-α observed in the *plin*$^{-/-}$ mice offer one potential mechanism for a large number of these coordinated changes in gene expression. However, other transcriptional factors and co-activators may also play a role, although candidate factors as other PPARs, nuclear respiratory factors, and PPAR-γ coactivator-1 were not significantly changed in the *plin*$^{-/-}$ mice. We further note that the absence of perilipin in the WAT also leads to concomitant changes in gene expression in other tissues where perilipin is not normally expressed. This reflects an intricate cross-talk between tissues. This cross-talk between tissues is likely to be mediated via the lipid ligands themselves or via secreted molecules such as adipocyte-derived cytokines and hormones. The identification of the mediator(s) for this cross-talk, however, awaits further study.

ACKNOWLEDGMENTS

This work was supported by a grant (HL-51586) from the National Institutes of Health to L.C. and by a grant (72570) from CONACyT, Mexico, to F.C.C. L.C. was also supported by the Betty Rutherford Chair in Diabetes Research at St. Luke's Episcopal Hospital and Baylor College of Medicine.

We thank Arturo Panduro for encouraging F.C.C. to pursue this work; Rainer Lanz for the use of the ABI Prism sequence detection system for the real-time PCR experiments; Benny Chang, Ke Ma, Susan Hilsenbeck, Patrick Younan, and Darin Tessier for technical advice; and Tracy Lynn Duncan and Leslie J. Wu for help in preparing the manuscript.

REFERENCES

1. Greenberg AS, Egan JJ, Wek SA, Moos MC Jr, Londos C, Kimmel AR: Isolation of cDNAs for perilipins A and B: sequence and expression of lipid droplet-associated proteins of adipocytes. *Proc Natl Acad Sci U S A* 90:12035–12039, 1993
2. Blanchette-Mackie EJ, Dwyer NK, Barber T, Coxey RA, Takeda T, Rondinone CM, Theodorakis JL, Greenberg AS, Londos C: Perilipin is located on the surface layer of intracellular lipid droplets in adipocytes. *J Lipid Res* 36:1211–1226, 1995
3. Londos C, Brasaemle DL, Schultz CJ, Adler-Wailes DC, Levin DM, Kimmel AR, Rondinone CM: On the control of lipolysis in adipocytes. *Ann N Y Acad Sci* 892:155–168, 1999
4. Greenberg AS, Egan JJ, Wek SA, Garty NB, Blanchette-Mackie EJ, Londos C: Perilipin, a major hormonally regulated adipocyte-specific phosphoprotein associated with the periphery of lipid storage droplets. *J Biol Chem* 266:11341–11346, 1991
5. Clifford GM, Londos C, Kraemer FB, Vernon RG, Yeaman SJ: Translocation of hormone-sensitive lipase and perilipin upon lipolytic stimulation of rat adipocytes. *J Biol Chem* 275:5011–5015, 2000
6. Zhang HH, Halbleib M, Ahmad F, Manganiello VC, Greenberg AS: Tumor necrosis factor-alpha stimulates lipolysis in differentiated human adipocytes through activation of extracellular signal-related kinase and elevation of intracellular cAMP. *Diabetes* 51:2929–2935, 2002
7. Martinez-Botas J, Anderson JB, Tessier D, Lapillonne A, Chang BH, Quast MJ, Gorenstein D, Chen KH, Chan L: Absence of perilipin results in leanness and reverses obesity in Lepr(db/db) mice. *Nat Genet* 26:474–479, 2000
8. Tansey JT, Sztalryd C, Gruia-Gray J, Roush DL, Zee JV, Gavrilova O, Reitman ML, Deng CX, Li C, Kimmel AR, Londos C: Perilipin ablation results in a lean mouse with aberrant adipocyte lipolysis, enhanced leptin production, and resistance to diet-induced obesity. *Proc Natl Acad Sci U S A* 98:6494–6499, 2001
9. Yechoor VK, Patti ME, Saccone R, Kahn CR: Coordinated patterns of gene expression for substrate and energy metabolism in skeletal muscle of diabetic mice. *Proc Natl Acad Sci U S A* 99:10587–10592, 2002
10. Li C, Wong WH: Model-based analysis of oligonucleotide arrays: expression index computation and outlier detection. *Proc Natl Acad Sci U S A* 98:31–36, 2001
11. Depre C, Shipley GL, Chen W, Han Q, Doenst T, Moore ML, Stepkowski S, Davies PJ, Taegtmeyer H: Unloaded heart in vivo replicates fetal gene expression of cardiac hypertrophy. *Nat Med* 4:1269–1275, 1998
12. Doniger SW, Salomonis N, Dahlquist KD, Vranizan K, Lawlor SC, Conklin BR: MAPPFinder: using Gene Ontology and GenMAPP to create a global gene-expression profile from microarray data. *Genome Biol* 4:R7, 2003
13. Dahlquist KD, Salomonis N, Vranizan K, Lawlor SC, Conklin BR: GenMAPP, a new tool for viewing and analyzing microarray data on biological pathways. *Nat Genet* 31:19–20, 2002
14. Moon YA, Shah NA, Mohapatra S, Warrington JA, Horton JD: Identification of a mammalian long chain fatty acyl elongase regulated by sterol regulatory element-binding proteins. *J Biol Chem* 276:45358–45366, 2001
15. Nakamura Y, Sakakibara J, Izumi T, Shibata A, Ono T: Transcriptional regulation of squalene epoxidase by sterols and inhibitors in HeLa cells. *J Biol Chem* 271:8053–8056, 1996
16. Matzno S, Yamauchi T, Gohda M, Ishida N, Katsuura K, Hanasaki Y, Tokunaga T, Itoh H, Nakamura N: Inhibition of cholesterol biosynthesis by squalene epoxidase inhibitor avoids apoptotic cell death in L6 myoblasts. *J Lipid Res* 38:1639–1648, 1997
17. Chugh A, Ray A, Gupta JB: Squalene epoxidase as hypocholesterolemic drug target revisited. *Prog Lipid Res* 42:37–50, 2003
18. Sonoda Y, Amano C, Endo M, Sato Y, Sekigawa Y, Fukuhara M: Lanosterol 14 alpha-demethylase (cytochrome P-45014DM): modulation of its enzyme activity by cholesterol feeding. *Biol Pharm Bull* 18:1009–1011, 1995
19. Trzaskos JM, Ko SS, Magolda RL, Favata MF, Fischer RT, Stam SH, Johnson PR, Gaylor JL: Substrate-based inhibitors of lanosterol 14 alpha-methyl demethylase: I. Assessment of inhibitor structure-activity relationship and cholesterol biosynthesis inhibition properties. *Biochemistry* 34:9670–9676, 1995
20. Stromstedt M, Rozman D, Waterman MR: The ubiquitously expressed human CYP51 encodes lanosterol 14 alpha-demethylase, a cytochrome P450 whose expression is regulated by oxysterols. *Arch Biochem Biophys* 329:73–81, 1996
21. Landschulz KT, Jump DB, MacDougald OA, Lane MD: Transcriptional control of the stearoyl-CoA desaturase-1 gene by polyunsaturated fatty acids. *Biochem Biophys Res Commun* 200:763–768, 1994
22. Kim HJ, Miyazaki M, Ntambi JM: Dietary cholesterol opposes PUFA-mediated repression of the stearoyl-CoA desaturase-1 gene by SREBP-1 independent mechanism. *J Lipid Res* 43:1750–1757, 2002
23. Miller CW, Waters KM, Ntambi JM: Regulation of hepatic stearoyl-CoA desaturase gene 1 by vitamin A. *Biochem Biophys Res Commun* 231:206–210, 1997
24. Lefevre P, Diot C, Legrand P, Douaire M: Hormonal regulation of stearoyl coenzyme-A desaturase 1 activity and gene expression in primary cultures of chicken hepatocytes. *Arch Biochem Biophys* 368:329–337, 1999
25. Miyazaki M, Ntambi JM: Role of stearoyl-coenzyme A desaturase in lipid metabolism. *Prostaglandins Leukot Essent Fatty Acids* 68:113–121, 2003
26. Ntambi JM: Regulation of stearoyl-CoA desaturase by polyunsaturated fatty acids and cholesterol. *J Lipid Res* 40:1549–1558, 1999
27. Kurebayashi S, Hirose T, Miyashita Y, Kasayama S, Kishimoto T: Thiazolidinediones downregulate stearoyl-CoA desaturase 1 gene expression in 3T3–L1 adipocytes. *Diabetes* 46:2115–2118, 1997
28. Kim YC, Gomez FE, Fox BG, Ntambi JM: Differential regulation of the stearoyl-CoA desaturase genes by thiazolidinediones in 3T3–L1 adipocytes. *J Lipid Res* 41:1310–1316, 2000
29. Miller CW, Ntambi JM: Peroxisome proliferators induce mouse liver stearoyl-CoA desaturase 1 gene expression. *Proc Natl Acad Sci U S A* 93:9443–9448, 1996
30. Casimir DA, Ntambi JM: cAMP activates the expression of stearoyl-CoA desaturase gene 1 during early preadipocyte differentiation. *J Biol Chem* 271:29847–29853, 1996
31. Falvella FS, Pascale RM, Gariboldi M, Manenti G, De Miglio MR, Simile MM, Dragani TA, Feo F: Stearoyl-CoA desaturase 1 (Scd1) gene overexpression is associated with genetic predisposition to hepatocarcinogenesis in mice and rats. *Carcinogenesis* 23:1933–1936, 2002
32. Park EI, Paisley EA, Mangian HJ, Swartz DA, Wu MX, O'Morchoe PJ, Behr SR, Visek WJ, Kaput J: Lipid level and type alter stearoyl CoA desaturase mRNA abundance differently in mice with distinct susceptibilities to diet-influenced diseases. *J Nutr* 127:566–573, 1997
33. Cohen P, Miyazaki M, Socci ND, Hagge-Greenberg A, Liedtke W, Soukas AA, Sharma R, Hudgins LC, Ntambi JM, Friedman JM: Role for stearoyl-CoA desaturase-1 in leptin-mediated weight loss. *Science* 297:240–243, 2002
34. Ntambi JM, Miyazaki M, Stoehr JP, Lan H, Kendziorski CM, Yandell BS, Song Y, Cohen P, Friedman JM, Attie AD: Loss of stearoyl-CoA desaturase-1 function protects mice against adiposity. *Proc Natl Acad Sci U S A* 99:11482–11486, 2002
35. Nakamura MT, Nara TY: Gene regulation of mammalian desaturases. *Biochem Soc Trans* 30:1076–1079, 2001
36. Tabor DE, Kim JB, Spiegelman BM, Edwards PA: Identification of conserved cis-elements and transcription factors required for sterol-regulated transcription of stearoyl-CoA desaturase 1 and 2. *J Biol Chem* 274:20603–20610, 1999
37. Shimomura I, Shimano H, Korn BS, Bashmakov Y, Horton JD: Nuclear sterol regulatory element-binding proteins activate genes responsible for the entire program of unsaturated fatty acid biosynthesis in transgenic mouse liver. *J Biol Chem* 273:35299–35306, 1998
38. Kim HJ, Miyazaki M, Man WC, Ntambi JM: Sterol regulatory element-binding proteins (SREBPs) as regulators of lipid metabolism: polyunsaturated fatty acids oppose cholesterol-mediated induction of SREBP-1 maturation. *Ann N Y Acad Sci* 967:34–42, 2002
39. Miyazaki M, Kim YC, Ntambi JM: A lipogenic diet in mice with a disruption of the stearoyl-CoA desaturase 1 gene reveals a stringent requirement of endogenous monounsaturated fatty acids for triglyceride synthesis. *J Lipid Res* 42:1018–1024, 2001
40. Soukas A, Cohen P, Socci ND, Friedman JM: Leptin-specific patterns of gene expression in white adipose tissue. *Genes Dev* 14:963–980, 2000

41. Sugden MC, Bulmer K, Holness MJ: Fuel-sensing mechanisms integrating lipid and carbohydrate utilization. *Biochem Soc Trans* 29:272–278, 2001
42. Wu P, Blair PV, Sato J, Jaskiewicz J, Popov KM, Harris RA: Starvation increases the amount of pyruvate dehydrogenase kinase in several mammalian tissues. *Arch Biochem Biophys* 381:1–7, 2000
43. Wu P, Sato J, Zhao Y, Jaskiewicz J, Popov KM, Harris RA: Starvation and diabetes increase the amount of pyruvate dehydrogenase kinase isoenzyme 4 in rat heart. *Biochem J* 329:197–201, 1998
44. Brun T, Assimacopoulos-Jeannet F, Corkey BE, Prentki M: Long-chain fatty acids inhibit acetyl-CoA carboxylase gene expression in the pancreatic beta-cell line INS-1. *Diabetes* 46:393–400, 1997
45. Kersten S, Mandard S, Tan NS, Escher P, Metzger D, Chambon P, Gonzalez FJ, Desvergne B, Wahli W: Characterization of the fasting-induced adipose factor FIAF, a novel peroxisome proliferator-activated receptor target gene. *J Biol Chem* 275:28488–28493, 2000
46. Krieger-Brauer HI, Kather H: Antagonistic effects of different members of the fibroblast and platelet-derived growth factor families on adipose conversion and NADPH-dependent H_2O_2 generation in 3T3 L1-cells. *Biochem J* 307:549–556, 1995
47. Soukas A, Socci ND, Saatkamp BD, Novelli S, Friedman JM: Distinct transcriptional profiles of adipogenesis in vivo and in vitro. *J Biol Chem* 276:34167–34174, 2001
48. Charriere G, Cousin B, Arnaud E, Andre M, Bacou F, Penicaud L, Casteilla L: Preadipocyte conversion to macrophages: evidence of plasticity. *J Biol Chem* 2003
49. Chen JS, Greenberg AS, Tseng YZ, Wang SM: Possible involvement of protein kinase C in the induction of adipose differentiation-related protein by Sterol ester in RAW 264.7 macrophages. *J Cell Biochem* 83:187–199, 2001
50. Faber BC, Cleutjens KB, Niessen RL, Aarts PL, Boon W, Greenberg AS, Kitslaar PJ, Tordoir JH, Daemen MJ: Identification of genes potentially involved in rupture of human atherosclerotic plaques. *Circ Res* 89:547–554, 2001